

Observation of a new charmonium-like state produced in association with a J/ψ in e^+e^- annihilation at $\sqrt{s} \approx 10.6$ GeV

K. Abe,⁷ I. Adachi,⁷ H. Aihara,⁴⁰ K. Arinstein,¹ Y. Asano,⁴⁴ V. Aulchenko,¹ T. Aushev,¹¹ T. Aziz,³⁶ A. M. Bakich,³⁵ V. Balagura,¹¹ M. Barbero,⁶ I. Bedny,¹ U. Bitenc,¹² I. Bizjak,¹² A. Bondar,¹ M. Bračko,^{7, 18, 12} J. Brodzicka,²⁵ T. E. Browder,⁶ Y. Chao,²⁴ A. Chen,²² B. G. Cheon,² R. Chistov,¹¹ S.-K. Choi,⁵ Y. Choi,³⁴ Y. K. Choi,³⁴ A. Chuvikov,³⁰ S. Cole,³⁵ J. Dalseno,¹⁹ M. Danilov,¹¹ M. Dash,⁴⁵ A. Drutskoy,³ S. Eidelman,¹ D. Epifanov,¹ S. Fratina,¹² N. Gabyshev,¹ T. Gershon,⁷ G. Gokhroo,³⁶ B. Golob,^{17, 12} H. C. Ha,¹⁴ J. Haba,⁷ Y. Hasegawa,³³ K. Hayasaka,²⁰ H. Hayashii,²¹ M. Hazumi,⁷ L. Hinz,¹⁶ Y. Hoshi,³⁸ S. Hou,²² W.-S. Hou,²⁴ Y. B. Hsiung,²⁴ T. Iijima,²⁰ A. Ishikawa,⁷ M. Iwasaki,⁴⁰ Y. Iwasaki,⁷ P. Kapusta,²⁵ T. Kawasaki,²⁷ H. R. Khan,⁴¹ H. J. Kim,¹⁵ S. M. Kim,³⁴ K. Kinoshita,³ S. Korpar,^{18, 12} P. Krokovny,¹ C. C. Kuo,²² A. Kuzmin,¹ J. S. Lange,⁴ G. Leder,¹⁰ T. Lesiak,²⁵ A. Limosani,⁷ S.-W. Lin,²⁴ D. Liventsev,¹¹ F. Mandl,¹⁰ T. Matsumoto,⁴² A. Matyja,²⁵ Y. Mikami,³⁹ W. Mitaroff,¹⁰ H. Miyata,²⁷ R. Mizuk,¹¹ Y. Nagasaka,⁸ E. Nakano,²⁸ M. Nakao,⁷ S. Nishida,⁷ O. Nitoh,⁴³ S. Ogawa,³⁷ T. Ohshima,²⁰ S. Okuno,¹³ S. L. Olsen,⁶ H. Ozaki,⁷ P. Pakhlov,¹¹ H. Palka,²⁵ C. W. Park,³⁴ H. Park,¹⁵ K. S. Park,³⁴ L. S. Peak,³⁵ L. E. Piilonen,⁴⁵ A. Poluektov,¹ Y. Sakai,⁷ N. Sato,²⁰ T. Schietinger,¹⁶ O. Schneider,¹⁶ A. J. Schwartz,³ R. Seidl,³¹ K. Senyo,²⁰ M. E. Sevier,¹⁹ B. Shwartz,¹ V. Sidorov,³ A. Somov,³ R. Stamen,⁷ M. Starič,¹² T. Sumiyoshi,⁴² S. Y. Suzuki,⁷ F. Takasaki,⁷ N. Tamura,²⁷ M. Tanaka,⁷ Y. Teramoto,²⁸ X. C. Tian,²⁹ K. Trabelsi,⁶ T. Tsukamoto,⁷ S. Uehara,⁷ T. Uglov,¹¹ K. Ueno,²⁴ Y. Unno,⁷ S. Uno,⁷ P. Urquijo,¹⁹ G. Varner,⁶ K. E. Varvell,³⁵ S. Villa,¹⁶ C. C. Wang,²⁴ C. H. Wang,²³ M.-Z. Wang,²⁴ E. Won,¹⁴ Q. L. Xie,⁹ B. D. Yabsley,⁴⁵ A. Yamaguchi,³⁹ Y. Yamashita,²⁶ M. Yamauchi,⁷ J. Ying,²⁹ C. C. Zhang,⁹ J. Zhang,⁷ L. M. Zhang,³² Z. P. Zhang,³² and V. Zhilich¹

(The Belle Collaboration)

¹*Budker Institute of Nuclear Physics, Novosibirsk*

²*Chonnam National University, Kwangju*

³*University of Cincinnati, Cincinnati, Ohio 45221*

⁴*University of Frankfurt, Frankfurt*

⁵*Gyeongsang National University, Chinju*

⁶*University of Hawaii, Honolulu, Hawaii 96822*

⁷*High Energy Accelerator Research Organization (KEK), Tsukuba*

⁸*Hiroshima Institute of Technology, Hiroshima*

⁹*Institute of High Energy Physics, Chinese Academy of Sciences, Beijing*

¹⁰*Institute of High Energy Physics, Vienna*

¹¹*Institute for Theoretical and Experimental Physics, Moscow*

¹²*J. Stefan Institute, Ljubljana*

¹³*Kanagawa University, Yokohama*

¹⁴*Korea University, Seoul*

¹⁵*Kyungpook National University, Taegu*

¹⁶*Swiss Federal Institute of Technology of Lausanne, EPFL, Lausanne*

¹⁷*University of Ljubljana, Ljubljana*

¹⁸*University of Maribor, Maribor*

¹⁹*University of Melbourne, Victoria*

²⁰*Nagoya University, Nagoya*

²¹*Nara Women's University, Nara*

²²*National Central University, Chung-li*

²³*National United University, Miao Li*

²⁴*Department of Physics, National Taiwan University, Taipei*

²⁵*H. Niewodniczanski Institute of Nuclear Physics, Krakow*

²⁶*Nippon Dental University, Niigata*

²⁷*Niigata University, Niigata*

²⁸*Osaka City University, Osaka*

²⁹*Peking University, Beijing*

³⁰*Princeton University, Princeton, New Jersey 08544*

³¹*RIKEN BNL Research Center, Upton, New York 11973*

³²*University of Science and Technology of China, Hefei*

³³*Shinshu University, Nagano*

³⁴*Sungkyunkwan University, Suwon*

³⁵*University of Sydney, Sydney NSW*

³⁶*Tata Institute of Fundamental Research, Bombay*

³⁷*Toho University, Funabashi*

³⁸*Tohoku Gakuin University, Tagajo*

³⁹*Tohoku University, Sendai*

⁴⁰*Department of Physics, University of Tokyo, Tokyo*

⁴¹*Tokyo Institute of Technology, Tokyo*

⁴²*Tokyo Metropolitan University, Tokyo*

⁴³*Tokyo University of Agriculture and Technology, Tokyo*

⁴⁴*University of Tsukuba, Tsukuba*

⁴⁵*Virginia Polytechnic Institute and State University, Blacksburg, Virginia 24061*

We report the first observation of a new charmonium-like state at a mass of $(3.943 \pm 0.006 \pm 0.006) \text{ GeV}/c^2$. This state, which we denote as $X(3940)$, is observed in the spectrum of masses recoiling from the J/ψ in the inclusive process $e^+e^- \rightarrow J/\psi + \text{anything}$. We also observe its decay into $D^*\bar{D}$ and determine its intrinsic width to be less $52 \text{ MeV}/c^2$ at the 90% C.L. These results are obtained from a 357 fb^{-1} data sample collected with the Belle detector near the $\Upsilon(4S)$ resonance, at the KEKB asymmetric-energy e^+e^- collider.

PACS numbers: 13.66.Bc, 12.38.Bx, 14.40.Gx

Recently there have been a number of reports of new charmonium or charmonium-like states: $\eta_c(2S)$ [1], $X(3872)$ [2], $Y(3940)$ [3] and $Y(4260)$ [4]. The latter three states have not been assigned to any charmonium states in the conventional quark model. Moreover, charmonium production in different processes is not well understood. One striking example is the surprisingly large cross section for double charmonium production in e^+e^- annihilation observed by Belle [5] and confirmed by BaBar [6]. These experimental results have generated renewed theoretical interest in the spectroscopy, decays and production of charmonium.

In this paper we report the observation of a new charmonium-like state above $D\bar{D}$ threshold, $X(3940)$, produced in the process $e^+e^- \rightarrow J/\psi X(3940)$. We also present results from searches for $X(3940)$ decay into $D\bar{D}$, $D^*\bar{D}$ and $J/\psi\omega$. The data used for this analysis correspond to an integrated luminosity of 357 fb^{-1} collected by the Belle detector at the $\Upsilon(4S)$ resonance and nearby continuum at the KEKB asymmetric-energy e^+e^- collider.

The J/ψ reconstruction procedure is identical to our previously published analyses [5, 7]. Oppositely charged tracks that are positively identified as muons or electrons are used for $J/\psi \rightarrow \ell^+\ell^-$ reconstruction. A partial correction for final state radiation and bremsstrahlung energy loss is performed by including the four-momentum of every photon detected within a 50 mrad cone around the electron direction in the e^+e^- invariant mass calculation. The two lepton candidate tracks are required to have a common vertex, with a distance from the interaction point in the plane perpendicular to the beam axis smaller than 1 mm. The $J/\psi \rightarrow \ell^+\ell^-$ signal region is defined by the mass window $|M_{\ell^+\ell^-} - M_{J/\psi}| < 30 \text{ MeV}/c^2$ ($\approx 2.5\sigma$). J/ψ candidates in the signal window are subjected to a mass and vertex constrained fit to improve

their momentum resolution. QED processes are substantially suppressed by requiring the total charged multiplicity (N_{ch}) in the event to be greater than four. Background due to J/ψ mesons produced from $B\bar{B}$ events is removed by requiring the center-of-mass (CM) momentum $p_{J/\psi}^*$ to be greater than $2.0 \text{ GeV}/c$. As in the previous analysis, we define the recoil mass as

$$M_{\text{recoil}}(J/\psi) = \sqrt{(E_{\text{CMS}} - E_{J/\psi}^*)^2 - p_{J/\psi}^{*2}}, \quad (1)$$

where $E_{J/\psi}^*$ is the J/ψ CM energy after the mass constraint.

For the study of the $X(3940) \rightarrow D^{(*)}\bar{D}$, we reconstruct D^0 candidates using five decay modes: $K^-\pi^+$, K^-K^+ , $K^-\pi^-\pi^+\pi^+$, $K_S^0\pi^+\pi^-$ and $K^-\pi^+\pi^0$; and D^+ candidates using $K^-\pi^+\pi^+$, $K^-K^+\pi^+$ and $K_S^0\pi^+$. For the $D^0 \rightarrow K^-\pi^-\pi^+\pi^+$ and $D^0 \rightarrow K^-\pi^+\pi^0$ modes, mass windows of $\pm 10 \text{ MeV}/c^2$ and $\pm 20 \text{ MeV}/c^2$ are used; a $\pm 15 \text{ MeV}/c^2$ mass window is used for all other modes (approximately 2.5σ in each case). To improve their momentum resolution, D candidates are refitted to the nominal D^0 or D^+ masses. To study the contribution of combinatorial background under the D peak, we use D sidebands with mass windows that are four times as large. For the $X(3940) \rightarrow J/\psi\omega$ search, candidate ω mesons are reconstructed from $\pi^+\pi^-\pi^0$ combinations within $\pm 20 \text{ MeV}/c^2$ ($\sim 2.5\sigma$) of the nominal ω mass. The ω sideband region is defined by $30 < |M(\pi^+\pi^-\pi^0) - M_\omega| < 50 \text{ MeV}/c^2$.

The recoil mass spectrum for the inclusive J/ψ event sample is shown in Fig. 1. Here, in addition to the three previously reported peaks at the η_c , χ_{c0} and $\eta_c(2S)$ masses, there is a fourth peak above $D\bar{D}$ threshold. We perform a fit to this spectrum that includes the three previously seen charmonium states plus a fourth state with mass near $3.94 \text{ GeV}/c^2$. The expected signal line-shapes are determined from Monte Carlo (MC) simulation as described in previous Belle publications [5, 7].

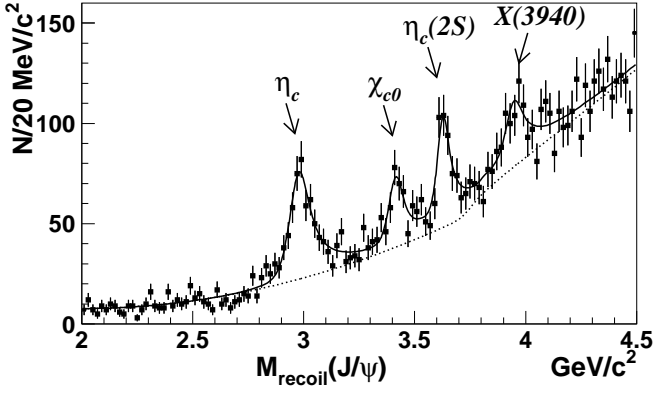


FIG. 1: The distribution of masses recoiling against the reconstructed J/ψ in inclusive $e^+e^- \rightarrow J/\psi X$ events. The curves are described in the text.

The mass values for the η_c , χ_{c0} , $\eta_c(2S)$ and $X(3940)$ are free parameters in the fit, the widths of η_c and χ_{c0} are fixed to PDG values [8] and the $\eta_c(2S)$ width is fixed to $\Gamma = 17 \text{ MeV}/c^2$ [9]. The width of the new state is a free parameter in the fit. The signal function for the $X(3940)$ is a convolution of the (zero-width) MC line shape with a Breit-Wigner function. The background is parameterized by a second order polynomial and a threshold term ($\sqrt{M_{\text{recoil}}(J/\psi) - 2M_D}$) to account for a possible contribution from $e^+e^- \rightarrow J/\psi D^{(*)}\bar{D}^{(*)}$.

The fit results are given in Table I. The significance for each signal is defined as $\sqrt{-2 \ln(\mathcal{L}_0/\mathcal{L}_{\text{max}})}$, where \mathcal{L}_0 and \mathcal{L}_{max} denote the likelihoods returned by the fits with the signal yield fixed at zero and at the fitted value, respectively. The significance of the $X(3940)$ signal is 5.0σ . The fitted width of the $X(3940)$ state is consistent with zero within its large statistical error: $\Gamma = 39 \pm 26 \text{ MeV}/c^2$. The fit results are shown in Fig. 1 as the solid curve; the dashed curve is the background function.

TABLE I: Summary of the signal yields, charmonium masses and significances for $e^+e^- \rightarrow J/\psi (c\bar{c})_{\text{res}}$.

$(c\bar{c})_{\text{res}}$	N	$M [\text{GeV}/c^2]$	N_σ
η_c	501 ± 44	2.970 ± 0.005	15.3
χ_{c0}	230 ± 40	3.406 ± 0.007	6.3
$\eta_c(2S)$	311 ± 42	3.626 ± 0.005	8.1
$X(3940)$	266 ± 63	3.936 ± 0.014	5.0

The new state has a mass that is above both the $D\bar{D}$ and $D^*\bar{D}$ thresholds. We therefore perform a search for $X(3940)$ decays into $D\bar{D}$ and $D^*\bar{D}$ final states. Because of the small product of $D^{(*)}$ reconstruction efficiencies and branching fractions, it is not feasible to reconstruct fully the chain $e^+e^- \rightarrow J/\psi X(3940)$, $X(3940) \rightarrow D^{(*)}\bar{D}$. To increase the efficiency, only one D meson

in the event is reconstructed in addition to the reconstructed J/ψ and the other \bar{D} or \bar{D}^* is detected as a peak in the spectrum of masses recoiling against the $J/\psi D$ combination. The Monte Carlo simulation for $e^+e^- \rightarrow J/\psi D\bar{D}$ and $e^+e^- \rightarrow J/\psi D^*\bar{D}$ processes indicates a $M_{\text{recoil}}(J/\psi D)$ resolution of about $30 \text{ MeV}/c^2$ and a separation between these two processes of 2.5σ . Figure 2 shows the $M_{\text{recoil}}(J/\psi D)$ spectrum in the D mass window (points with error bars) and in the scaled D mass sidebands (hatched histogram), where D includes D^0 and D^+ . Some events have multiple D candidates. In these cases, only the candidate with invariant mass closest to the nominal D -meson mass is used. Two peaks around the nominal D and D^* masses are clearly visible in this distribution. The excess of real D events compared to the D sidebands at masses above $2.1 \text{ GeV}/c^2$ is due to $e^+e^- \rightarrow J/\psi D^*\bar{D}^*$ or $e^+e^- \rightarrow J/\psi D^{(*)}\bar{D}^{(*)}\pi$ processes. A fit to this spectrum is performed using shapes fixed from MC for three processes ($J/\psi D\bar{D}$, $J/\psi D^*\bar{D}$ and $J/\psi D^*\bar{D}^*$) and a second order polynomial. The fit

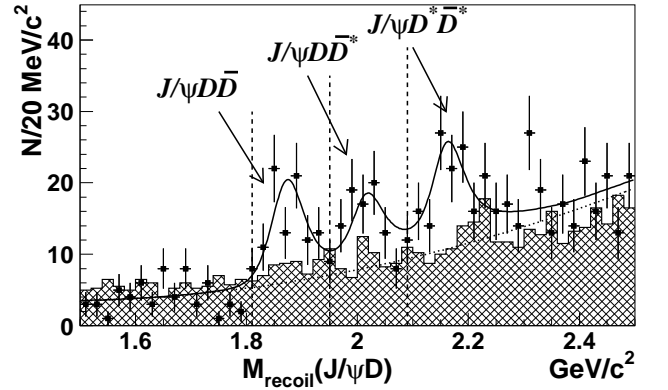


FIG. 2: The distribution of masses recoiling against the reconstructed $J/\psi D$ combinations in the data. Points with error bars correspond to the D mass signal window; hatched histograms show the scaled D sideband contribution. The solid line represents the fit described in the text. The dashed line shows the background function.

gives $N_{D\bar{D}} = 86 \pm 17$ (5.1σ) and $N_{D^*\bar{D}} = 55 \pm 18$ (3.3σ) events in the D and the D^* peaks, respectively. Selecting events from the $M_{\text{recoil}}(J/\psi D)$ regions around the D and D^* masses ($\pm 70 \text{ MeV}/c^2$), we thus effectively tag the processes $e^+e^- \rightarrow J/\psi D\bar{D}$ and $e^+e^- \rightarrow J/\psi D^*\bar{D}$.

We constrain $M_{\text{recoil}}(J/\psi D)$ to the $D^{(*)}$ nominal mass, thereby improving the $M(D^{(*)}\bar{D}) \equiv M_{\text{recoil}}(J/\psi)$ resolution by a factor of 2.5 ($\sigma \sim 10 \text{ MeV}/c^2$ after constraint), according to the MC simulation. In the $X(3940) \rightarrow D^*\bar{D}$ case, the reconstructed D can be from either the $X(3940)$ decays or the D^* decay: the constraint $M_{\text{recoil}}(J/\psi D) \rightarrow M(D^*)$ also works in the latter case, as both $X(3940) \rightarrow D^*\bar{D}$ and D^* decays have very little available phase space.

The resulting $M_{\text{recoil}}(J/\psi)$ distributions are shown in

Figs. 3a) ($M(D)$ region) and 3b) ($M(D^*)$ region). The cross-hatched histograms show the scaled D sideband distributions. For events with multiple entries, the candidate with invariant mass closest to the nominal D -meson mass (for D signal window) or closest to the center of the sideband (for sidebands) is used. An

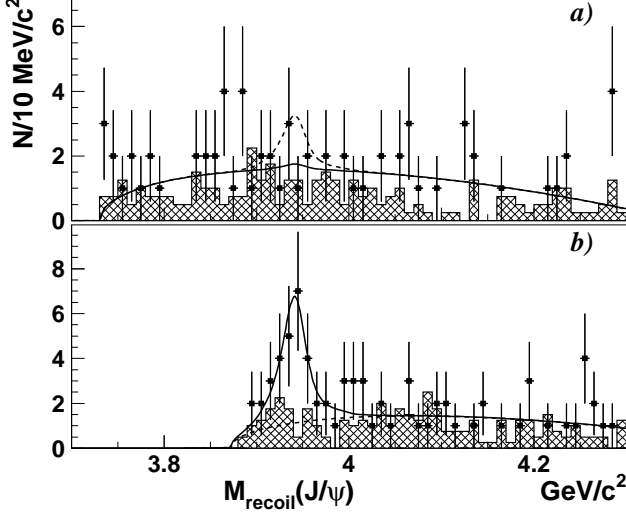


FIG. 3: The $M_{\text{recoil}}(J/\psi)$ distribution for events tagged and constrained as a) $e^+e^- \rightarrow J/\psi D\bar{D}$, and b) $e^+e^- \rightarrow J/\psi D^*\bar{D}$. The hatched histograms correspond to scaled D sidebands. The solid lines are result of the fits, described in the text. The dashed lines show: a) the 90% C.L. upper limit on the signal; b) the background function.

$X(3940)$ peak with a resolution that is better than that for the unconstrained $M_{\text{recoil}}(J/\psi)$ distribution is evident in Fig. 3b), corresponding to the decay $X(3940) \rightarrow D^*\bar{D}$. We perform a fit to this distribution. The signal function is a convolution of a Breit-Wigner with a free width and a resolution function fixed to the MC expectation. The background function is a threshold function $(A + B \cdot M(D^*\bar{D}))\sqrt{M(D^*\bar{D}) - M_{\text{thr}}}$ with $M_{\text{thr}} \equiv M(D^*) + M(D)$. The fit yields the number of signal events in the peak $N = 24.5 \pm 6.9$ with a statistical significance of 5.0σ . The width of the $X(3940)$ is $\Gamma = (15.4 \pm 10.1) \text{ MeV}/c^2$. The mass of the state is measured to be $M = (3.943 \pm 0.006) \text{ GeV}/c^2$.

We perform a similar fit to the $M_{\text{recoil}}(J/\psi)$ distribution for events tagged and constrained as $e^+e^- \rightarrow J/\psi D\bar{D}$. Since no $X(3940)$ signal is seen for this mode, we fit this distribution with $X(3940)$ parameters fixed to the values found by the fit of tagged $e^+e^- \rightarrow J/\psi D^*\bar{D}$. The signal yield is found to be $0.2^{+4.4}_{-3.5}$ events and we set an upper limit for the $X(3940)$ signal of 8.1 events at the 90% C.L.

An enhancement with a similar mass, $Y(3940)$, decaying into $J/\psi\omega$ has been recently observed by Belle [3] in B decays. We perform a search for the decay $X(3940) \rightarrow J/\psi\omega$ to see if $X(3940)$ and $Y(3940)$ could be the same

particle. To increase the efficiency we reconstruct the ω and only one J/ψ from the $J/\psi J/\psi\omega$ final state. The unreconstructed J/ψ is identified as a peak in the spectrum of recoil masses against the reconstructed $J/\psi\omega$ combinations. A signal for $X(3940) \rightarrow J/\psi\omega$ would be seen as a peak around the nominal $X(3940)$ mass in a distribution of $M_{\text{recoil}}(J/\psi) - M_{\text{recoil}}(J/\psi\omega) + M(J/\psi)$ if the reconstructed J/ψ is prompt, and in the $J/\psi\omega$ invariant mass distribution if the reconstructed J/ψ is from the $X(3940)$ decay. Since the first case has much larger combinatorial background and less sensitivity, we use only the second case. A scatterplot of $M_{\text{recoil}}(J/\psi\omega)$ vs. $J/\psi\omega$ invariant mass in the data is shown in Fig. 4a). An $M(J/\psi\omega)$ projection with the additional requirement $|M_{\text{recoil}}(J/\psi\omega) - M_{J/\psi}| < 100 \text{ MeV}/c^2$ is shown in Fig. 4b). A fit to this distribution is done with the signal function and parameters fixed from the result of the $D^*\bar{D}$ tagged fit; the background is a threshold function. The fit yields $1.9^{+3.2}_{-2.4}$ signal events corresponding to a 7.4 event upper limit at the 90% C.L.

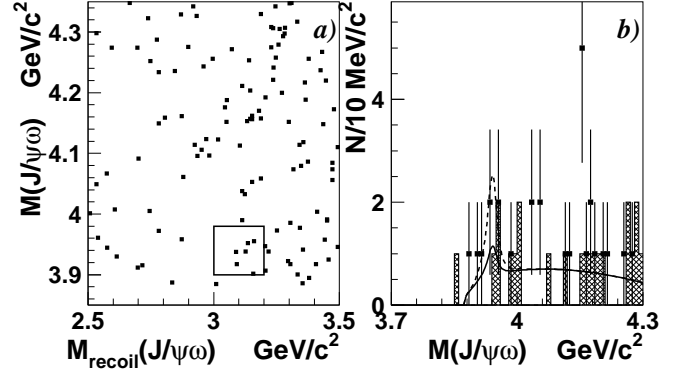


FIG. 4: a) The scatterplot of $M_{\text{recoil}}(J/\psi\omega)$ vs. $M(J/\psi\omega)$, and projection onto b) $M(J/\psi\omega)$. Points with error bars show the contribution from the ω mass window; the hatched histogram shows the ω sideband. The solid line represents the fit described in the text and the dashed line the 90% C.L. upper limit on the $X(3940) \rightarrow J/\psi\omega$ contribution.

The systematic errors for the $e^+e^- \rightarrow J/\psi X(3940)$ Born cross section and for the $X(3940)$ branching fractions $\mathcal{B}(X(3940))$ are summarized in Table II. To estimate the systematic errors associated with the fitting procedure we study the difference in $X(3940)$ yield returned by the fit to the $M_{\text{recoil}}(J/\psi)$ distribution under different assumptions for the signal and background parameterization. In particular, in the first fit we use a background function that includes several threshold functions corresponding to the production of $D^*\bar{D}$ and $D^*\bar{D}^*$. We also use the threshold function $(A + B \cdot M_{\text{recoil}}(J/\psi))\sqrt{M_{\text{recoil}}(J/\psi) - M_{\text{thr}}}$. Different angular distributions result in different J/ψ (and D) reconstruction efficiencies. In the MC the J/ψ production angle and J/ψ , $X(3940)$ helicity angle distributions are assumed

TABLE II: Contribution to the systematic error for $\sigma_{\text{Born}}(e^+e^- \rightarrow J/\psi X(3940))$ and $\mathcal{B}(X(3940))$ [%].

Source	σ_{Born}	$\mathcal{B}(X(3940))$		
		$D^*\bar{D}$	$D\bar{D}$	$J/\psi\omega$
Fitting procedure	± 11	± 17	—	—
Angular distributions	± 19	± 12	± 12	± 16
N_{ch} requirement	± 3	± 3	± 3	± 3
Reconstruction	± 2	± 6	± 6	± 5
Identification	± 3	± 1	± 1	—
Total	± 23	± 22	± 14	± 17

to be flat. The possible extreme angular distributions ($1 + \cos^2 \theta$ and $\sin^2 \theta$) are considered to estimate the systematic uncertainty of this assumption. This uncertainty partially cancels out in the determination of $\mathcal{B}(X(3940))$ because of the common J/ψ efficiency. Other contributions come from $N_{\text{ch}} > 4$ requirement efficiency, track reconstruction efficiency, lepton identification for reconstructed J/ψ and kaon identification for reconstructed D .

The systematic errors in the measurement of the $X(3940)$ mass are dominated by the $5 \text{ MeV}/c^2$ uncertainty associated with the fitting procedure. The uncertainty due to the J/ψ momentum scale is less than $3 \text{ MeV}/c^2$ [7]. These contributions are added in quadrature to give $6 \text{ MeV}/c^2$ total. The systematic error on the mass of the nearby $\eta_c(2S)$, which is still poorly known [8], is found to be the same. From the fit to Fig. 3b) we estimate the $X(3940)$ width to be smaller than $47 \text{ MeV}/c^2$ at the 90% C.L.; this takes into account the fact that the likelihood function is not parabolic. When fitting systematics are taken into account, we find $\Gamma < 52 \text{ MeV}/c^2$ at the 90% C.L.

The Born cross section for $e^+e^- \rightarrow J/\psi X(3940)$ is calculated following the procedure used in Ref. [7]. As in the previous Belle papers, because of selection criteria the result is presented in terms of the product of the cross section and the branching fraction of the $X(3940)$ into more than two charged tracks ($\mathcal{B}_{>2}$). We obtain

$$\sigma_{\text{Born}} \times \mathcal{B}_{>2} = (10.6 \pm 2.5 \pm 2.4) \text{ fb}. \quad (2)$$

Using the $X(3940)$ yields in inclusive and $D^*\bar{D}$ tagged samples, we calculate the fraction of $X(3940)$ decays with more than two charged tracks in the final state into $D^*\bar{D}$, $\mathcal{B}_{>2}(X(3940) \rightarrow D^*\bar{D})$. To remove the correlation between the two samples, we apply a veto on $D^*\bar{D}$ tagging in the inclusive sample. Correcting for the tagging and veto efficiencies obtained from MC with equal fractions of $X(3940) \rightarrow D^{*0}\bar{D}^0$ and $X(3940) \rightarrow D^{*+}D^-$ assumed, we find

$$\mathcal{B}_{>2}(X(3940) \rightarrow D^*\bar{D}) = (96^{+45}_{-32} \pm 22)\% \quad (> 45\% \text{ at } 90\% \text{ C.L.}), \quad (3)$$

where the systematic errors are taken into account for the lower limit. In the limit of a vanishing fraction of low charged multiplicity $X(3940)$ decays, the measured value of $\mathcal{B}_{>2}$ corresponds to $\mathcal{B}(X(3940) \rightarrow D^*\bar{D})$.

We set upper limits on the branching fractions of decay of $X(3940)$ into $D\bar{D}$ and $X(3940) \rightarrow J/\psi\omega$ final states, taking into account the estimated systematic errors:

$$\mathcal{B}(X(3940) \rightarrow D\bar{D}) < 41\% \text{ at } 90\% \text{ C.L.}; \quad (4)$$

$$\mathcal{B}(X(3940) \rightarrow J/\psi\omega) < 26\% \text{ at } 90\% \text{ C.L.} \quad (5)$$

These limits assume that low charged multiplicity $X(3940)$ decays are negligible and, thus, may be overestimated.

In summary, we have observed a new charmonium-like state, $X(3940)$, produced in the process $e^+e^- \rightarrow J/\psi X(3940)$, both in inclusive production and via the $X(3940) \rightarrow D^*\bar{D}$ decay mode. Both observations have a 5σ statistical significance. We have measured the Born cross section for the production process, the branching fraction for $X(3940) \rightarrow D^*\bar{D}$, and set upper limits on $X(3940)$ decays to $D\bar{D}$ and $J/\psi\omega$.

We thank the KEKB group for the excellent operation of the accelerator, the KEK cryogenics group for the efficient operation of the solenoid, and the KEK computer group and the NII for valuable computing and SuperSINET network support. We acknowledge support from MEXT and JSPS (Japan); ARC and DEST (Australia); NSFC (contract No. 10175071, China); DST (India); the BK21 program of MOEHRD and the CHEP SRC program of KOSEF (Korea); KBN (contract No. 2P03B 01324, Poland); MIST (Russia); MHEST (Slovenia); SNSF (Switzerland); NSC and MOE (Taiwan); and DOE (USA).

-
- [1] S.K. Choi *et al.* (Belle Collaboration), Phys. Rev. Lett. **89**, 102001 (2002).
 - [2] S.K. Choi *et al.* (Belle Collaboration), Phys. Rev. Lett. **91**, 262001 (2003).
 - [3] S.K. Choi *et al.* (Belle Collaboration), Phys. Rev. Lett. **94**, 182002 (2005).
 - [4] B. Aubert *et al.* (BaBar Collaboration), Phys. Rev. Lett. **95**, 142001 (2005).
 - [5] K. Abe *et al.* (Belle Collaboration), Phys. Rev. Lett. **89**, 142001 (2002).
 - [6] B. Aubert *et al.* (BaBar Collaboration), Phys. Rev. **D 72**, 031101 (2005).
 - [7] K. Abe *et al.* (Belle Collaboration), Phys. Rev. **D70**, 071102 (2004).
 - [8] S. Eidelman *et al.* (Particle Data Group), Phys. Lett. **B592**, 1 (2004).
 - [9] B. Aubert *et al.* (BaBar Collaboration), Phys. Rev. Lett. **92**, 142002 (2004).